Article No. jmbi.1999.2726 available online at http://www.idealibrary.com on IDEAL® J. Mol. Biol. (1999) 289, 57–67

JMB

Biophysical Analysis of the Interaction of Human Ifnar2 Expressed in *E. coli* with IFNα2

Jacob Piehler and Gideon Schreiber*

Department of Biological Chemistry, The Weizmann Institute of Science, Rehovot 76100 Israel

**Corresponding author*

Type I interferons are cytokines which activate an anti-viral response by binding to two specific cell surface receptors, ifnar1 and ifnar2. Here, we report purification and refolding of the extracellular part of human ifnar2 (ifnar2-EC) expressed in *Escherichia coli* and its characterization with respect to its interaction with interferon α2 (IFNα2). The 25 kDa, non-glycosylated ifnar2-EC is a stable, fully active protein, which inhibits anti-viral activity of IFNα2. The stoichiometry of binding IFNα2 is 1:1, as determined by gel filtration, chemical cross-linking and solid-phase detection. The affinity of this interaction is 10 nM, which is similar to the affinity measured for the cell surface-bound ifnar2 receptor. No difference in affinity was found throughout various assays using optical detection as BIAcore or reflectometric interference spectorscopy. However, the binding kinetics as measured in homogeneous phase by fluorescence dequenching was about three times faster than that measured on a sensor surface. The rate of complex formation is relatively high compared to other cytokine-receptor interactions. The salt dependence of the association kinetics suggest a limited but significant contribution of electrostatic forces towards the rate of complex formation. The dissociation constant increases with decreasing pH according to the protonation of a base with a pK_a of 6.7. The surface properties of the IFNα2 binding surface on ifnar2 were interpreted according to the pH and salt dependence of the interaction.

Keywords: IFNα; Ifnar2; kinetics; heterogeneous-phase-detection; electrostatics

Introduction

Interferons are cytokines initially characterized by their potent anti-viral activity. Human type I interferons include a large family of about 13 different IFNα functional non-allelic genes (with 70% homology between them), a single gene encoding for IFNβ (35% homology to IFNα) as well as IFNω and τ. Two cellular receptors are involved in binding all type I interferons, ifnar1 (Uzè *et al.*, 1990) and ifnar2 (Novick *et al.*, 1994). Mutagenesis studies have suggested that the binding site for each of the two receptors is located at a different part of the interferon molecule (Uzè *et al.*, 1995). Upon binding, interferon causes the two receptors to associate, with interferon bridging them together (Cohen *et al.*, 1995). In addition to ifnar1 and ifnar2, their associated intracellular tyrosine kinases (Tyk2 and Jak1) are also required for the productive presentation of the binding site (Uzè *et al.*, 1995). Three molecular forms of ifnar2 are generated by alternative splicing: a soluble secreted protein and two transmembrane forms. All three have identical extracellular (EC) domains (Domanski *et al.*, 1995; Novick *et al.*, 1994). The binding affinity of the ternary ifnar1-ifnar2-IFNα2 complex is in the numomolara range, with ifnar2 alone binding IFNα2 at a five- to tenfold lower affinity (Cohen *et al.*, 1995; Cutrone & Langer, 1997). ifnar1 alone does not seem to be able to bind either IFNα2 or IFNβ at a detectable level (Cohen *et al.*, 1995; Cutrone & Langer, 1997; Langer *et al.*, 1998). No structures are available for ifnar1 or ifnar2, but it is possible to model ifnar2 according to its homology to the known structures of TF receptor, HGH-R and IFN-γ-R (Lewerenz *et al.*, 1998).

Abbreviations used: IFN, interferon; ifnar1, ifnar2, type I interferon receptor 1 and 2; EC, extracellular part; SPR, surface plasmon resonance; HBS, Hepes-buffered saline; RU, refractive index unit; RIfS, reflectometric interference spectroscopy.

E-mail address of the corresponding author: bcges@wiccmail.weizmann.ac.il

0022-2836/99/210057–11 $30.00/0

However, one has to be cautious regarding to the accuracy of the model, as the homology between these proteins is below 25 %, with the lowest homology being near the suggested binding site of interferon on ifnar2, which was determined by mutagenesis studies (Lewerenz *et al*., 1998).

A detailed understanding of the protein-protein interactions which initiate the interferon signaling pathway requires accurate structural information. For such investigations, large amounts of pure and active protein are required. The ability to express proteins heterologously in *Escherichia coli* had a big impact on the study of structure-function relation on a number of other cytokines, as for example HGH-receptor (de Vos *et al*., 1992), TF-receptor (Harlos *et al*., 1994) and interferon-γ-receptor interactions (Walter *et al*., 1995). All those three receptor molecules are cell surface glycoproteins (as is ifnar2). Still, their binding activity and structure does not seem to be affected by the loss of glycosylation upon expression in *E. coli*.

Here, we describe for the first time the successful refolding and purification of the extracellular domain of ifnar2 (ifnar2-EC) expressed in *E. coli*, and its characterization in terms of its ability to bind interferon. We assessed the kinetics and thermodynamics of this interaction using biological and biophysical methods, including anti-viral protection cell assays, analytical gel filtration, optical heterogeneous phase detection and fluorescence spectroscopy. We show that the non-glycosilated extracellular portion of ifnar2 is a soluble protein, which retains the ability to bind IFNα2 with a 1:1 stoichiometry with the same affinity as the natural cell surface receptor.

Results

The extracellular domain of ifnar2 (ifnar2-EC) and IFNα2 were expressed in *E. coli* under the control of a T7 promoter in a modified pT7T318U vector, to which we added a two-cistron translational initiation site. The advantage of this expression system is that it eliminates problems related to translational activation of heterologous expression in *E. coli* without the use of a fusion-protein. The use of this vector improved the otherwise poor expression of ifnar2-EC (Figure 1, lane 1). All ifnar2-EC protein precipitated in the form of inclusion bodies (lanes 2 and 3) which were solubilized in 8 M urea. SDS-PAGE analysis under non-reducing conditions (lane 4) revealed that about 50 % of the protein were monomeric, while the rest formed multimeric, disulfide-linked aggregates. Refolding was initiated by a 20-fold dilution. The monomeric fraction of ifnar2-EC was extracted from this solution by batch ion exchange chromatography. Further purification by column ion-exchange was necessary to remove other species of ifnar2-EC, which were monomeric, but inactive, as well as other proteins (lane 5 and 6). After gel filtration chromatography, ifnar2-EC was purified

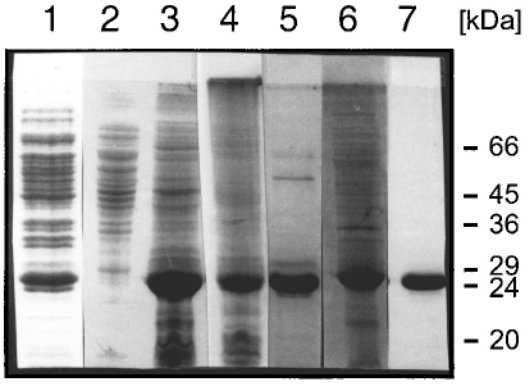

Figure 1. Expression and purification of ifnar2-EC in *E. coli*: cells harvested four hours after induction of protein expression (lane 1). The cell content was fractionated to soluble (lane 2) and insoluble inclusion bodies. Inclusion bodies solubilized in 8 M urea (lane 3: +DTT; lane 4: no DTT). Active (lane 5) and inactive (lane 6) fractions of ifnar2-EC were separated by ion-exchange chromatography. After a step of gel filtration ifnar2-EC is of at least 95 % homogeneity (lane 7).

to at least 95 % homogeneity (lane 7). Typical protein yields were 2.5 mg/l cell culture. A single, sharp band at 25 kDa was observed in SDS-PAGE both under reducing and non-reducing conditions (cf. Figure 4, lane 2). N-terminal sequencing of ifnar2-EC showed that the protein starts at residues SYDSP, in agreement with the expected sequence. The protein sequencing assay also confirmed a level of purification of at least 95 %. Ellman assays under native and denaturing conditions clearly proved that properly folded ifnar2-EC does not contain free cysteine residues. Hence, three disulfide bonds are formed in the mature protein.

Anti-viral and neutralization activity of recombinant IFNα2 and ifnar2-EC

An antiviral activity of 8×10^8 units/mg was measured by a cytopathic effect inhibition assay in human WISH cells for the *E. coli*-produced IFNα2, using NIH IFNβ as a standard. This is in the typical range found for IFNα2 from other sources. A 50 % inhibition of the activity of 25 units/ml (1.6×10^{-12} M) of IFNα2 was observed with 10 nM ifnar2-EC. Concentrations of ifnar2-EC higher than 100 nM completely inhibited the activity of IFNα2 in this assay. A dissociation constant of 1.1×10^{-8} M for the interaction between ifnar2-EC and IFNα2 was determined by fitting equation (1) to the residual IFNα2 activity upon titration with ifnar2-EC (Figure 2).

Stoichiometry of ifnar2-EC-IFNα2 binding

Analytical size-exclusion chromatography was used to evaluate the fraction of active protein as well as to determine the stoichiometry of the

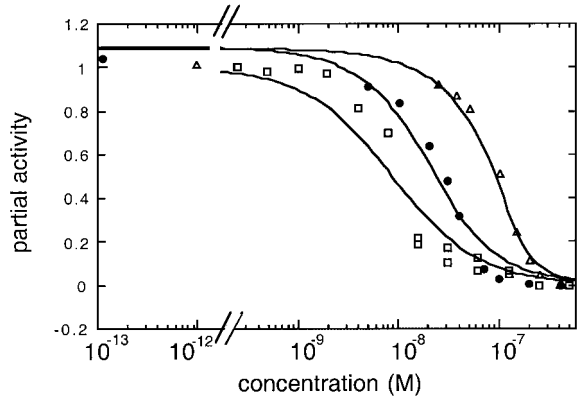

Figure 2. Binding of ifnar2-EC to IFNα2 measured in homogeneous phase by binding inhibition assays: (□) inhibition of anti-viral activity of IFNα2 on WISH cell. IFNα2 concentration was 1.6×10^{-12} M. The other two curves are of binding inhibition assays, where residual ifnar2-EC concentrations are monitored by optical heterogeneous phase detection with immobilized IFNα2: (△) by RIfS with a constant IFNα2 concentration of 150 nM; (●) BIAcore with a constant IFNα2 concentration of 20 nM.

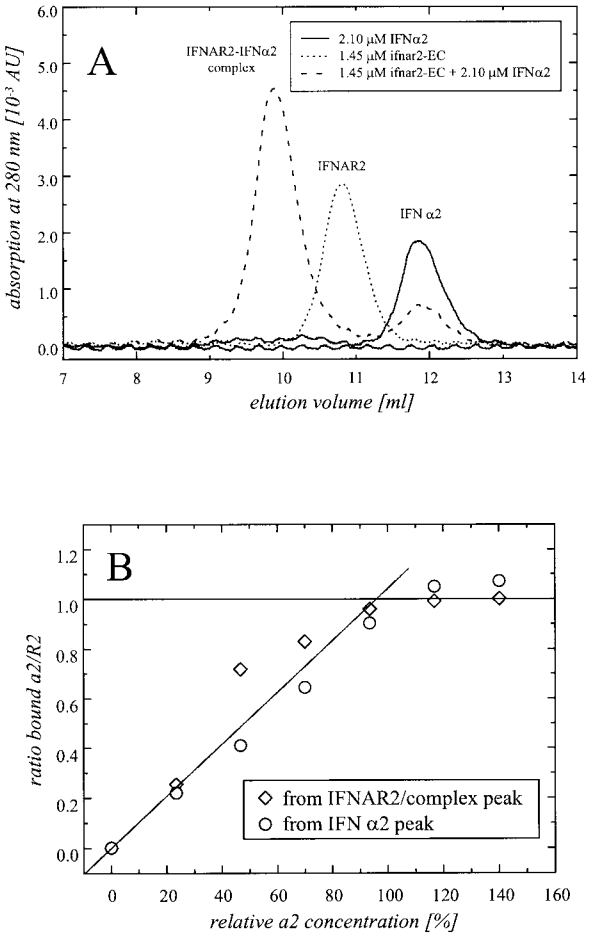

Figure 3. Binding of IFNα2 with ifnar2-EC monitored by analytical gel filtration. (a) Gel-filtration chromatograms at different relative stoichiomentries (Superdex^R 75 HR 10/30 column). The concentrations of the proteins used in each run are shown in the legend. (b) Stoichiometry of binding of ifnar2-EC with IFNα2 as determined from gel filtration. The contributions of IFNα2 and ifnar2-EC to the complex were determined by integration of the peak areas, corrected by the extinction coefficients of the two proteins.

complex. Figure 3(a) shows the chromatograms of IFNα2, ifnar2-EC and the complex formed by these two proteins at different concentrations. On this column (Superdex^R 75 HR10/30), free IFNα2 eluted at a volume of 12 ml, ifnar2-EC at 10.8 ml and the complex of the two at 9.8 ml. Keeping the concentration of ifnar2-EC constant and increasing the relative concentration of IFNα2 resulted in a diminishing peak of the non-bound ifnar2-EC, while the peak of the complex increased. The peak representing the complex reached its maximum at a 1:1 stoichiometry of IFNα2:ifnar2-EC, and did not further increase upon increasing the quantity of IFNα2. At excess IFNα2, a further peak appeared, which corresponds to the non-bound protein. A quantitative analysis of the area under the three peaks clearly shows that the stoichiometry of the complex observed under these conditions is 1:1 (Figure 3(b)). Molecular mass standards further corroborated the size of the complex (data not shown). A stoichimetric excess of one of the proteins resulted in a complete disappearance of the peak of the other protein, supporting the evidence that both IFNα2 and ifnar2-EC were more than 95% active. No dissociation of the complex was observed during the run in the column. The protein concentration in the column was about 100-200 nM, supporting the evidence that the affinity between the two proteins is at least in the lower nanomolar range.

Further validation of the 1:1 stoichiometry of the interaction between IFNα2 and ifnar2-EC in μM concentration was obtained by zero-length cross-linking of the two proteins. The analysis of the cross-linked species by SDS-PAGE are shown in Figure 4. The non-cross-linked complex (lane 3) shows the two bands of IFNα2 (lane 1) and ifnar2-EC (lane 2). Upon adding the cross-linking reagent (EDC) to IFNα2 (lane 4) or to ifnar2-EC (lane 5) no changes were detected. However, when applying the reagent to the complex, an additional species of the size of 45 kDa appeared (lane 6). This size exactly corresponds to the sum of the molecular mass of IFNα2 and ifnar2-EC. No other species were detected for this cross-linking method.

Characterization of the IFNα2-ifnar2-EC interaction with optical biosensor systems

Investigation of the interaction of proteins by label-free solid phase detection such as surface plasmon resonance (SPR) or reflectometric interference spectroscopy (RIfS) requires the immobilization of one of the interacting compounds. We

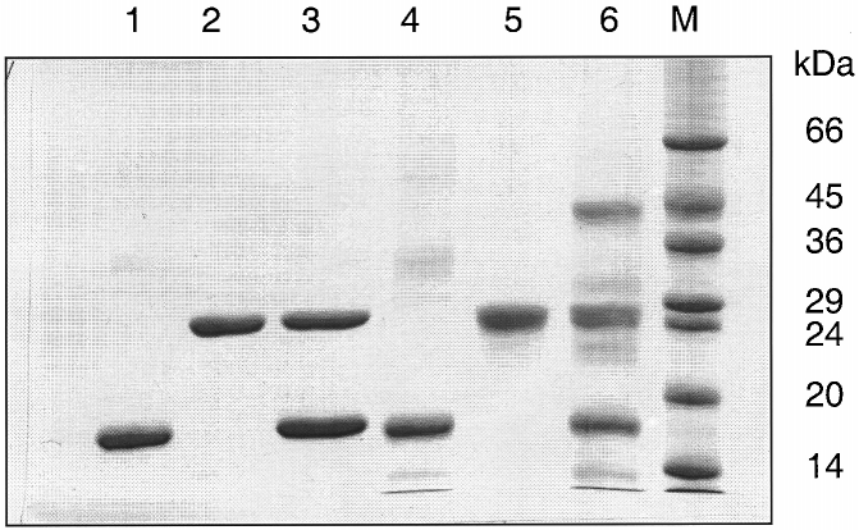

Figure 4. Analysis of the chemically cross-linked proteins by SDS-PAGE: lanes 1-3 represent the non-cross-linked proteins IFNα2 (lane 1), ifnar2-EC (lane 2) and the complex (lane 3). Lanes 4-6 represent the proteins after cross-linking: IFNα2 (lane 4) ifnar2-EC (lane 5) and the complex (lane 6).

have employed both of these techniques using covalent immobilization of both IFNα2 and ifnar2-EC *via* free amine groups into a carboxylated dextran layer. Most of the investigations were carried out by RIfS, with the results corresponding very well to results obtained by SPR on a BIAcore2000. All results are summarized in Table 1.

IFNα2 reacted readily with the activated surface leading to irreversible attachment of approximately 50 % of the pre-concentrated protein within 400 seonds. Subsequent injections of ifnar2-EC in various concentration revealed that typically 30 % of the bound IFNα2 was active, i.e. can bind ifnar2-EC. The immobilized protein was stable at room temperature for several days (20 % loss of activity per day), without significant loss of activity when treated with 100 mM HCl. Binding of ifnar2-EC (Figure 5) to the immobilized IFNα2 was clearly specific and was completely inhibited when adding an excess of free IFNα2. The dissociation of the complex at the surface was fitted by a single exponential decay, with the residuals of the fit distributed randomly around zero. At pH 7.4 and 150 mM NaCl, a mean dissociation rate constant k_{off} of 0.035 (±0.003) s^{-1} was consistently observed, independent on the time range used for fitting. The value of k_{off} is constant between pH 7.4 and 9, but increases rapidly at lower pH values (Figure 6) down to approximately 0.1 s^{-1} at pH 5.5. A pK_a value of 6.7 was determined from this dependency by fitting a model that assumed two distinct dissociation rate constants for the two differently charged states of the protein interface.

Several problems where encountered during the evaluation of the binding of ifnar2-EC to immobilized IFNα2. (i) The association phase deviates significantly from a first-order kinetic model. Therefore, only the first 25 seconds of the binding curve could be used to extract the association rate constant. (ii) The values of the association rate constants decreased with ligand concentration. As a result the observed rate of association (k_s) did not show a linear dependence on ligand concentration (Figure 7(a)). (iii) The equilibrium surface loading R_{eq} is not a hyperbolic function of the concentration, which is revealed by the non-linearity of

Table 1. Binding constants for the association of IFNα2 with ifnar2-EC

Methods of measurement		Immobilized	k_{on} ($\times 10^{-6}$) ($M^{-1,}$ s^{-1})	k_{off} (s^{-1})	K_d^a (nM)	K_d^b (nM)
RIfS	Heterogeneous	IFNα2	0.2 (0.15)	0.035 (0.003)	190 (150)	35 (11)
RIfS	Heterogeneous	ifnar2-EC	2.3 (0.15)	0.022 (0.002)	10 (1)	12 (1.5)
RIfS	Homogeneous	IFNα2				10 (2.5)
BIAcore	Heterogeneous	IFNα2		0.032 (0.001)		160 (30)
BIAcore	Heterogeneous	ifnar2-EC	2.2 (0.3)	0.017 (0.002)	8 (1.5)	
BIAcore	Homogeneous	IFNα2				10 (3)
Stopped-flow fluorescence	Homogeneous		7.1 (0.5)			
Anti-viral neutralization	Homogeneous					11 (2.5)

All measurements were performed in 50 mM Hepes (pH 7.4) and 150 mM NaCl. In heterogeneous phase one of the proteins was bound to the sensor surface, while in homogeneous phase both proteins were in solution. Affinity constants in homogeneous phase were determined by equilibrium titration in solution using the immobilized protein to probe the equilibrium free concentration of the other protein (Piehler *et al.*, 1997). Numbers in parenthesis are either the standard deviations (σ) determined from at least five repeated measurements or the standard errors determined from a curve fit of at least five independent measurements.

[a] K_d is calculated from k_{off}/k_{on} measured in heterogeneous phase.

[b] K_d is determined from equilibrium response in either homogeneous or heterogeneous phase (see Figures 2, 5 and 7).

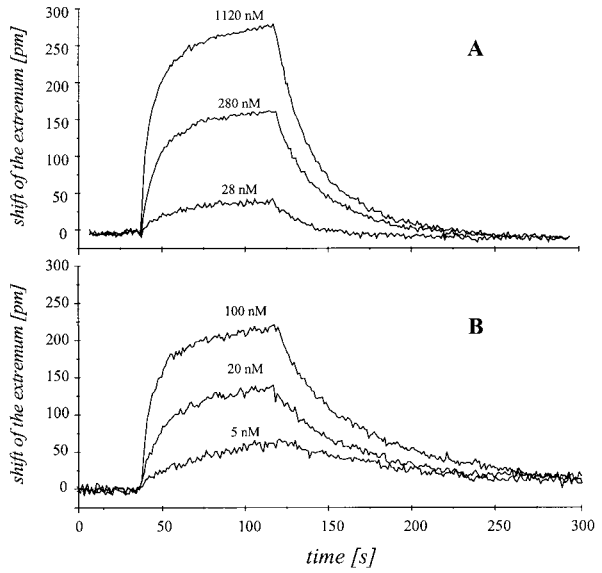

Figure 5. Interaction of ifnar2-EC and IFNα2 measured with RIfS. (a) ifnar2-EC at different concentrations binding to immobilized IFNα2; (b) IFNα2 at different concentrations binding to immobilized ifnar2-EC.

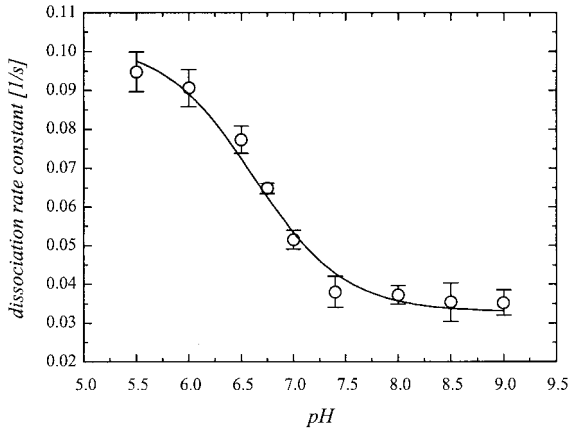

Figure 6. pH dependence of the dissociation rate constant of ifnar2-EC and IFNα2 measured by RIfS. The line corresponds to a model that was fit to the data assuming a distinct dissociation rate constant for each of two states of ionization.

the Scatchard-plot (Figure 7(b)). Therefore, no consistent affinity information can be extracted by this method.

ifnar2-EC reacted with a high degree of efficiency with the surface, but specific activity was only 5-10 % of the total surface loading. The ifnar2-EC bound to the surface was loosing about 50 % of its activity per day and 100 % activity upon treatment with 100 mM HCl. Nevertheless, specific binding of IFNα2 to immobilized ifnar2-EC was clearly detectable with a typical maximum surface loading R_{max} of 100-150 pm (100 - 150 pg/mm^2).

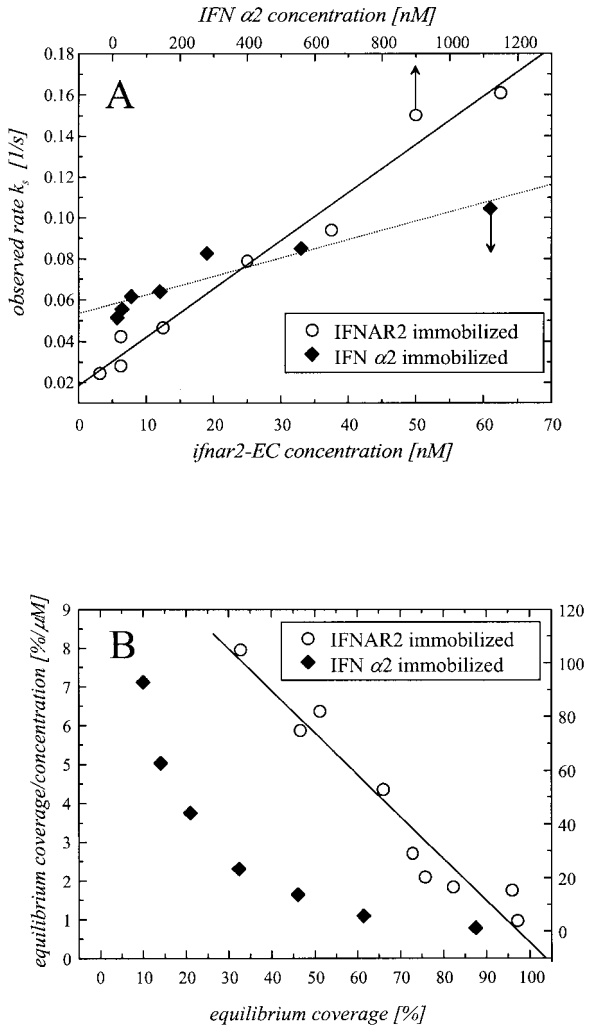

Figure 7. Kinetic and equilibrium analysis of the interaction of ifnar2-EC and IFNα2 measured by RIfS. (a) Observed rate constant k_s *versus* the concentration; (b) Scatchard-plot determined from the equilibrium surface loading observed for immobilized IFNα2 and ifnar2-EC. For comparison, the equilibrium surface loading R_{eq} is normalized by the maximum surface loading R_{max}.

This corresponds to a surface concentration of active ifnar2-EC of 5-10 pmol/mm^2. Dissociation followed a single exponential kinetics leading to a dissociation rate constant of 0.022 s^{-1}, which is about 30 % lower than that observed for the immobilized IFNα2. However, the association phase of the binding curve gave consistent results in this constellation. No systematic deviations from the pseudo-first-order kinetics model were observed, with an average association rate constant of 2.3×10^6 M^{-1} s^{-1} for all IFNα2 concentrations. The plot of the observed association rate k_s *versus* the concentration (Figure 7(a)) gave a linear correlation. The rate constants determined by linear regression were in excellent agreement with the rate constants determined from the individual curves (Table 1). A dissociation constant K_d of

10 nM was obtained from these rate constants assuming $K_d = k_{off}/k_{on}$. Evaluation of the equilibrium response in a Scatchard-plot gave a single dissociation constant of 12.5 nM (Figure 7(b)). The values from all these evaluation methods including their errors are compared in Table 1. As this is the first time that RIfS technology was used to monitor interactions with covalently attached proteins, we validated this data by comparing them with data obtained in similar conditions using a BIAcore 2000 with a standard CM5 chip. No significant differences (2σ criterion, $\alpha = 0.95$) were found between the rate constants measured with RIfS *versus* the BIAcore (Table 1).

Heterogeneous phase detection can also be used for determining affinity constants in solution by a binding inhibition assay (Piehler *et al.*, 1997). The principle of this method is similar to the inhibition assay of anti-viral activity of IFNα2. In both cases, the equilibrium concentration of free protein in solution is detected by its binding to the immobilized protein, either on the cell surface or on the transducer surface. We used this approach for characterizing the interaction between IFNα2 and ifnar2-EC by immobilizing IFNα2 to the surface, and titrating ifnar2-EC in solution with increasing concentrations of IFNα2. Concentration of free ifnar2-EC was determined from the residual binding to the immobilized IFNα2. The titration curves obtained for two ifnar2-EC concentrations are shown in Figure 2. By fitting the accurate binding model obtained from the law of mass action (equation (2)) to the data, a dissociation constant K_d of 10 nM was obtained for both concentrations.

Interaction kinetics in solution

Fluorescence spectra of the free proteins and of the complex at an excitation wavelength of 280 nm revealed that de-quenching of tryptophane fluorescence occurs upon binding (data not shown). Dequenching of the fluorescence allowed measurement of the association rate constant in solution using a stopped-flow technique. Under pseudo-first-order conditions, an association rate constant of $7 \times 10^6\ M^{-1}\,s^{-1}$ was determined for complex formation in 150 mM NaCl at pH 7.4 (Figure 8(a)). This is three times higher than the association rate constant measured at the solid-liquid interface with immobilized ifnar2-EC. Assuming that under the experimental conditions no intermediate accumulates during the association reaction, the dissociation rate constant in solution is $0.07\ s^{-1}$.

The contribution of electrostatic steering can be estimated from the electrostatic energy of interaction of the two proteins in the transition state (U_{el}). Analyzing the dependence of the association rate constant on salt concentration revealed a linear relation between $\ln k_{on}$ and $(1 + \kappa a)^{-1}$ (Figure 8(b)). Linear regression gave a slope of 4, which is a measure of the electrostatic energy contribution U_{el}/RT to the association rate constant. The basal association rate constant in the absence of electrostatic forces is $8 \times 10^5\ M^{-1}s^{-1}$ as determined from the intercept of the plot (infinite ionic strength).

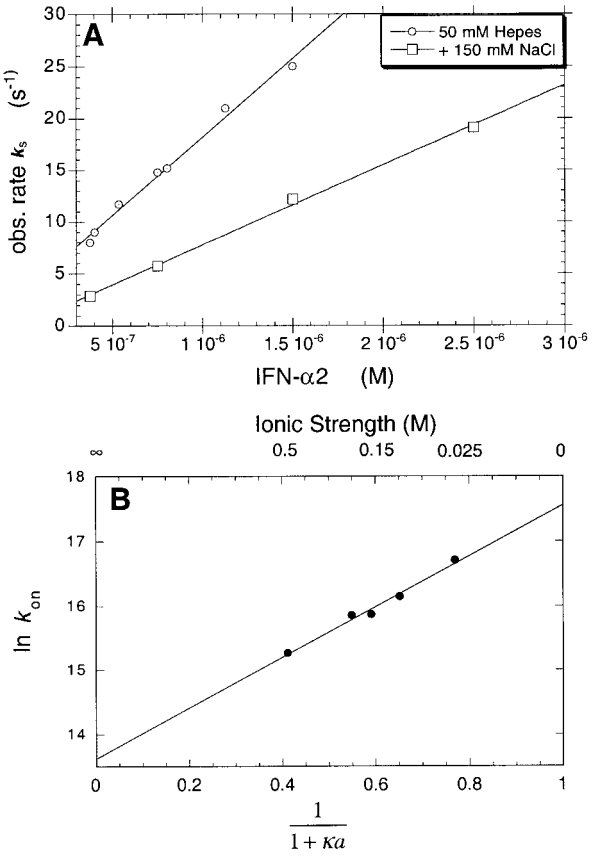

Figure 8. Determination of the association rate constant in solution by monitoring fluorescence de-quenching in a stopped flow. (a) Association rate constants in solution were determined from the slope of the linear dependence of the rate of association measured in a stopped-flow, plotted *versus* protein concentration. (b) The electrostatic contribution to the rate of association is estimated from the dependence of $\ln k_{on}$ on salt concentration. Salt concentrations are transformed to $(1 + \kappa a)^{-1}$, where κ is the inverse of the Debye-length and a is the minimal distance of approach set to 6 Å. The slope of the curve gives the electrostatic energy contribution U_{el}/RT of the association reaction.

Discussion

A prerequisite for biophysical studies of proteins is the ability to express, refold and purify them in large quantities while retaining the activity of the original proteins. Here, we have described refolding, purification and extensive characterization of the extracellular part of the human type I interferon receptor ifnar2 (ifnar2-EC) expressed in *E. coli*. Recombinant ifnar2-EC was found to be a very stable protein with all cysteine residues forming intra-molecular disulfide bonds. Its activity as an inhibitor of type I interferons is similar to the original p40 ifnar2-

EC purified from human urine (Novick *et al*., 1994). Applying the 2σ criterion ($\alpha = 0.95$), the binding affinity of 10 nM to IFNα2 was found consistently throughout various assays. This dissociation constant does not significantly differ from those reported for cell surface-bound and soluble human ifnar2 (Cohen *et al*., 1995; Cutrone & Langer, 1997). From these results we conclude that the non-glycosylated ifnar2-EC described in this study has essentially retained its biological activity and can be used for further biophysical investigations of the type I interferon receptor. This is not surprising, as several other extracellular domains of cytokine receptors have been expressed successfully in *E. coli* (Bignon *et al*., 1994; Cacaccia *et al*., 1993; Fuh *et al*., 1990).

Ifnar2-EC was purified from the inclusion bodies of *E. coli*. However, we found that for about 50% of the total ifnar2-EC only intra-molecular disulfide bonds were formed. A total of 70% of this protein refolded into fully active ifnar2-EC, with the three disulfide bonds correctly formed. The remaining 50% ifnar2-EC formed disulfide linked, high molecular mass aggregates. The ratio of correctly formed disulfide bonds in the inclusion bodies is surprisingly high. Random formation of three correct disulfide bonds from an unfolded polypeptide chain is highly unlikely: we never found conditions to re-form the disulfide bonds *in vitro* after reduction. Oxidation of reduced ifnar2-EC always resulted in the formation of high molecular mass aggregates. We suggest that the protein was already properly folded in the reducing environment of the *E. coli* cytosol, prior to aggregation in inclusion bodies. This phenomenon has already been observed in our laboratory for the overexpression of BLIP (β-lactamase inhibitor protein) in *E.coli* (Albeck & Schreiber, 1999). Ellman assays confirmed that all six cysteine residues of ifnar2-EC form intramolecular disulfide bonds. Homology modeling based on tissue factor receptor suggests that the three disulfide bonds are between the cysteine residues 12:95, 58:66 and 178:200.

The interaction between ifnar2-EC and IFNα2 was analyzed both in homogeneous phase and at the solid-liquid interface by a variety of methods. The stoichiometry of binding in homogeneous phase was measured to be 1:1 for IFNα2 as determined from gel-filtration (100 nM concentrations) and chemical cross-linking (lower micromolar concentration). These results do not exclude the possibility that at higher concentrations weak interactions can lead to complexes of different stoichiometries. Surface-bound proteins can cluster to very high local concentrations. Heterogeneous phase detection mimics such conditions, allowing for real-time monitoring of binding. Here we immobilized ifnar2-EC (or IFNα2) to a very flexible dextran layer which would allow interaction of more than one ifnar2-EC with IFNα2 (as has been observed for human growth hormone binding to immobilized receptor; Cunningham & Wells, 1993). The ifnar2-EC concentration in the dextran layer is 5-10 pmol/mm^2, which corresponds to a receptor density of about 50000 per cell. Still, single-phase association and dissociation kinetics were observed at all surface loadings, and ligand concentrations, extending over the whole amplitude. Multiple-phasic association and dissociation curves are frequently seen when monitoring surface binding, and their interpretation needs caution because of experimental artifacts. This is not the case when only a single phase is observed. This can be interpreted as a single process occurring, which suggests a 1:1 stoichiometry for the interaction of IFNα2 with ifnar2-EC.

Heterogeneous phase detection offers a variety of approaches to characterize the kinetics and thermodynamics of binding. Still one has to view the results critically. Here we compare interaction parameters determined from immobilized IFNα2 or ifnar2-EC with measurements in homogeneous phase. Upon immobilization of IFNα2, single-phase dissociation kinetics with a uniform rate constant for all protein concentrations was observed. However, determined values of association rate constants and affinity varied with concentration. These results could be explained by the non-specific immobilization procedure, which may had affected the binding site of the immobilized IFNα2, leading to different interaction properties. However, because of the fast, single-phase dissociation kinetics, we tend to ascribe the reduced and inconsistent association kinetics of ifnar2-EC to the considerable electrostatic repulsion of ifnar2-EC (net charge of −13) by the negatively charged dextran layer in which IFNα2 is immobilized. A very similar phenomenon has been observed in our laboratory for the association of the negatively charged TEM-1-β-lactamase to immobilized BLIP (Albeck & Schreiber, 1999).

Binding of IFNα2 to immobilized ifnar2-EC gave consistent values of rate constants and affinity, independent on concentration. The same binding affinity was determined for IFNα2 binding to immobilized ifnar2-EC, as for complex formation in solution. Still, the association rate constant was three times lower with ifnar2-EC immobilized to the surface, compared to stopped-flow measurements in the homogeneous phase. This indicates that the dynamics of the interaction is affected by the immobilization of ifnar2-EC without affecting the free energy of the complex formation. This phenomenon has been frequently observed for solid phase detection of protein-protein interactions and has been ascribed to a variety of reasons. However, in case of a membrane anchored receptor like ifnar2, the kinetics obtained by solid phase detection may even more authentically reflect the biological processes on the cell surface.

The rate constants of association and dissociation between ifnar2-EC and IFNα2 are relatively high compared to other cytokine receptor interactions,

as for example IL-4-receptor ($k_{on} = 1.3 \times 10^7$ $M^{-1}s^{-1}$, $k_{off} = 2 \times 10^{-3}$ s^{-1} for a 1:1 interaction; Wang *et al.*, 1997), HGH-receptor ($k_{on} = 4x10^5$ $M^{-1}s^{-1}$ $k_{off} = 3x10^{-4}$ s^{-1} for a 1:1 interaction; Cunningham & Wells, 1993) or IL-6 - IL-6Rα ($k_{on} = 2.6 \times 10^5$ $M^{-1}s^{-1}k_{off} = 1x10^{-2}$ s^{-1} ; Toniatti *et al.*, 1996). The fast interaction dynamics could play an important role in signal transduction, as this means that the complex between IFNα2 and ifnar2 is short living, while retaining relative high affinity. This gives only a limited time for ifnar1 to associate into the active ternary complex. Fast transient kinetics also has methodological implications, because indirect affinity assays like binding inhibition and sequential solid phase detection can be strongly affected by fast dissociation. Therefore, monitoring of the interaction by fluorescence dequenching and real-time BIA is much more reliable for an accurate assessment of affinity. This becomes particular important for characterizing mutants, which are expected to have even higher dissociation rate constants.

The dependence of the interaction kinetics on ion strength and on the pH provides some insight into the properties of IFNα2 binding site of ifnar2. Electrostatic steering plays an important role in fast association of protein complexes (Schreiber & Fersht, 1996). It is generally found that the binding sites of two fast associating proteins are complementary charged. As the binding site of ifnar2 on IFNα2 is positively charged (Radhakrishnan *et al.*, 1996) and the surface of ifnar2-EC is strongly negatively charged, such electrostatic rate enhancement can be expected. However, the dependence of the association rate constant on the salt concentration revealed a rather high basal rate constant and only modest electrostatic enhancement. Thus, electrostatic forces play only a limited role in determining the rate of association for this complex, suggesting that the interferon binding site on ifnar2 is not at a negatively charged hot spot on the protein surface. This compares favorable with the electrostatic potential at the binding site of interferon on an ifnar2 structural model, as suggested from mutagenesis studies (Lewerenz *et al.*, 1998; J.P. & G. S., unpublished data). It will be interesting to see how electrostatic steering affects the association rate of other type I interferons to ifnar2.

The pH dependence of the dissociation rate constant attests the involvement of at least one histidine residue in the interaction between ifnar2-EC and IFNα2 with a pK_a of 6.7 in the complex. The rate of dissociation at pH 5.5 is nearly three times faster than at physiological pH, indicating lower affinity in case of a protonated, positively charged histidine residue. At least two histidine residues are located within the binding interface, one is His34 in IFNα2 (Radhakrishnan *et al.*, 1996) , and the other is His103 in ifnar2 (Lewerenz *et al.*, 1998). The lower affinity of the protonated species indicates a downshift of the pK_a in the complex compared to the free species. Hence, the pK_a of the histidine residue in the free protein is even higher than 6.7 and strongly up-shifted compared to the pK_a of a free histidine residue (6.3). This requires a negatively charged local environment (Loewenthal *et al.*, 1993) and therefore indicates that this histidine residue is on the ifnar2-EC surface. The tight pH dependence of the dissociation rate constant could be of biological significance and remains to be investigated more thoroughly.

The long-term goal of our investigations is a detailed understanding of the recognition of type I interferons by its receptor on the molecular level to decipher its structure-activity relationship. With the work presented in this study, we believe to have established a very solid and promising bases for this project: (i) an efficient procedure for preparation and purification of ifnar2-EC in large quantities which are required for crystallization and for investigations by NMR; and (ii) reliable methods for quantitatively assessing affinity and dynamics of the interaction. In particular solid phase detection with immobilized ifnar2-EC seems very useful for a rapid and accurate affinity screening required for a mutational mapping of the binding site. Additionally, this method can provide a better understanding of the interferon signaling by allowing us to simulate conditions on the cell surface and to monitor the processes at the interface in real time.

Experimental Procedures

Cloning of the extracellular part of the *ifnar2* gene into a two-cistron expression vector

The extracellular part of the ifnar2 gene (212 bp) from SYDSP (N-ter) to ESEFS (C-ter; Novick *et al.*, 1994) was amplified by PCR from the plasmid pCEV9 (given to us by M. Rubinstein). Upstream of serine 1 of *ifnar2* we added a *Nde*I restriction site, and downstream the C-terminal serine we added a TAA stop codon, followed by a *Sal*I restriction site. The *ifnar2* gene was cloned into a expression vector based on the pT7T3-18U plasmid, to which we added a second cistron just upstream from the starting codon. The second cistron is of the first nine amino acid residues of the *lpp* 5′ gene, including its SD site flanked by *Xba*I and *Nde*I restriction sites (for details on the sequence of the first cistron, see Schoner *et al.*, 1990). The reason for inserting a second cistron was to improve the yield of heterologous protein expression (Schoner *et al.*, 1990). The same protocol was used to construct an expression vector for IFNα2. The new expression vectors are called pT72CR2 (for ifnar2-EC) and pT72Cα2 (for IFNα2).

Expression and purification of recombinant ifnar2-EC from *E. coli*

For protein production, TG1 cells containing the pT72CR2 plasmid were grown at 37°C in 750 ml of 2 × TY medium containing 100 μg/ml ampicilin in two liter flasks. At $A_{600} = 0.6$, protein expression was induced by the addition of 0.2 mM IPTG and infection with M13/T7 phage at an MOI of five plaque forming units per cell (Invitrogen, the phage is expressing the T7 polymerase under the control of a lac promoter). After four hours of additional growth, the cells were pelleted and

resuspended in lysis buffer containing 100 mM Tris (pH 8.4), 100 mM NaCl, 1 mM EDTA and lysozyme (50 μg/ml). After sonication, the insoluble fraction was separated by centrifugation and the inclusion bodies were washed with lysis buffer which did not contain lysozyme. Inclusion bodies were dissolved by stirring in 8 M urea for one hour. The denatured protein was refolded by a 20-fold dilution into 100 mM Tris (pH 8.4). The proteins were extracted by adding a cationic ion-exchange resin (Q Sepharose^R Fast Flow; Pharmacia Biotech) to the solution for one hour and filtering the beads on a sintered glass funnel. After intensive washing, the protein was eluted with 0.5 M NaCl. The eluted protein was diluted fourfold and directly applied to an ion-exchange column (HiTrap Q, Pharmacia) with a gradient of 0-500 mM NaCl at pH 8.4. Fractions containing major amounts of ifnar2-EC were pooled and further purified by gel filtration on a Sephadex^R 75 column (16/26) in 50 mM Tris (pH 8.4) and 100 mM NaCl. All purification steps were analyzed by SDS-PAGE under reducing and non-reducing conditions.

Expression and purification of recombinant human IFNα2

The gene coding for IFNα2 was cloned into the two-cistron expression vector described for *ifnar2* yielding the plasmid pT72Cα2. To improve the level of expression, the codons for the first 23 amino acid residues were changed into: TGT GAT CTG CCG CAG ACT CAC TCT CTG GGT TCT CGT CGT ACT CTG ATG CTG CTG GCT CAG ATG CGT CGT. For protein expression, a similar protocol as for ifnar2-EC was followed. IFNα2 was found in the inclusion bodies, which were dissolved in 8 M urea containing 5 mM DTT. IFNα2 was refolded by a 20 fold dilution overnight. Protein purification was carried out as described for ifnar2-EC. Typical yields of protein were 10 mg/l cell culture. IFNα2 runs as a single band of 18 kDa on SDS-PAGE.

Determination of protein concentration

Extinction coefficients of $\varepsilon_{280} = 26{,}500$ for ifnar2-EC, and $\varepsilon_{280} = 18{,}070$ for IFNα2 were determined by the method by Gill & von Hippel (1989). Protein concentrations were determined from the UV absorbance at 280 nm using the appropriate extinction coefficients.

Anti-viral activity of IFNα2 and its inhibition by ifnar2-EC

The anti-viral activity of recombinant IFNα2 produced in *E. coli* was measured by inhibition of the cytopathic effect in human WISH cells using VSV as challenge virus (Rubinstein *et al.*, 1981), relative to NIH standard IFNβ. A binding inhibition assay of IFNα2 anti-viral activity was carried out with ifnar2-EC as follows: 25 units/ml (1.6×10^{-12} M) of IFNα2 were mixed with ifnar2-EC in a concentration range of 2.4×10^{-10} to 5×10^{-7} M and residual IFNα2 anti-viral activity was determined. IFNα2 activity was quantified by measuring the absorbance of light of crystal violet stained WISH cells in the ELISA plate. The corresponding concentration of free IFNα2 was determined by calibration of the IFNα2 activity at eight different concentrations between 5.4×10^{-14} M and 1.6×10^{-12} M on the same plate. The dissociation constant K_d was determined from the titration curve by fitting a simplified model derived from the law of mass action for the case that the concentration of IFNα2 is very small compared to the K_d:

$$\frac{c_{\alpha 2}}{c_{0,\alpha 2}} = \frac{K_d}{K_d + c_{0,R2}} \quad (1)$$

where c depicts the free concentration and c_0 the overall concentration of the species IFNα2 (index α2) and ifnar2-EC (index $R2$).

Analytical gel filtration

Protein purity and activity was monitored by analytical size-exclusion chromatography in a TSKgel QC-PAK GFC 200 column (TosoHaas) and a Superdex^R 75 HR10/30 column (Pharmacia Biotech). Protein samples of 120 μl with a protein concentration around 1 μM were injected *via* a 100 μl sample loop. The stoichiometry of the complex was determined by titration with increasing IFNα2 at a constant ifnar2-EC concentration of 1.45 μM. The area under the IFNα2 peak and the double peak of ifnar2-EC and the complex were determined by integration. The contribution of IFNα2 in the complex was calculated from the ifnar2-EC/complex peak by subtracting the area of the original free ifnar2-EC peak. The resulting peak areas were corrected by the extinction coefficients assuming unchanged absorption of the proteins in the complex, and normalized by the peak areas of the free ifnar2-EC to give relative concentrations. The relative concentration of IFNα2 in the complex peak was plotted *versus* the relative IFNα2 concentration added in the sample.

Chemical cross-linking

The IFNα2-ifnar2-EC complex was chemically cross-linked with the zero-length cross-linking reagent 1-ethyl-3-(3-dimethylaminopropyl) carbodiimide (EDC; Sigma). To 100 μl of a mixture of 8 μM ifnar2-EC and 6 or 12 μM IFNα2 in 10 mM Hepes (pH 7.4) and 100 mM NaCl, 1.5 μl of a freshly prepared 0.2 M aqueous solution of EDC was added. After fast mixing, the solution was incubated for five hours. As a control, a sample which contained either 8 μM recombinant ifnar2-EC or only 12 μM IFNα2 were treated with EDC exactly in the same way. The reaction was stopped by adding 20 μl of 1 M Tris-acetate (pH 7.8) and the samples were analyzed by SDS-PAGE under reducing conditions.

Biomolecular interaction analysis

The interaction between recombinant ifnar2-EC and IFNα2 was monitored by an optical probe called reflectometric interference spectroscopy (RIfS; Gauglitz *et al.*, 1993). This method detects biomolecular interaction at interfaces as a change of the apparent optical thickness of a thin silica layer and has been described in detail before (Gauglitz *et al.*, 1993; Schmitt *et al.*, 1997). Binding to the surface was monitored as a shift in the interference spectrum. A shift of 1 pm corresponds to approximately 1 pg/mm^2 protein on the surface. The transducer surface was modified with a dextran layer (Piehler *et al.*, 1996) and carboxylated by reaction with molten glutaric anhydride (Sigma) at 75 °C for two to eight hours. On such surfaces, electrostatic pre-concentration and covalent immobilization of proteins were carried out by standard BIAcore protocols. All measurements were carried out in

50 mM Hepes (pH 7.4), 150 mM NaCl and 0.01 % Triton X100. Measurements at different pH were carried out by adjusting the pH of this buffer to avoid possible artifacts due to different buffer ions. A sample volume of 800 µl was injected for 80 seconds, while sampling with a data acquisition rate of 1 Hz. By using flow rates up to 50 µl/s, the samples in the flow cell were exchanged within one second, allowing for analysis of processes occurring within ten seconds. The binding curves were evaluated with the BIAevaluation software (BIAcore AB, Sweden) using simple one-to-one kinetics models.

SPR measurements were performed on a BIAcore 2000 (BIAcore AB) using a CM5 chip with 300 RU (refractive index units) of active IFNα2 or 50 RU of active ifnar2-EC bound to the surface. Measurement were done under standard conditions in HBS (10 mM Hepes, 3.4 mM EDTA, 150 mM NaCl, 0.05 % surfactant P20, pH 7.4) at 25 °C (Cunningham & Wells, 1993; Karlsson *et al*., 1991).

Affinity constants were determined by equilibrium titration in solution using the immobilized protein to probe the equilibrium free concentration of the other protein (Piehler *et al*., 1997). In these titration experiments, the concentration of free ifnar2-EC was titrated with increasing concentrations of IFNα2 in solution and detected by monitoring the binding to immobilized IFNα2. The initial slopes of these binding curves, which correspond to the free IFNα2 concentration, were determined by an exponential fit and plotted *versus* the IFNα2 concentration. The affinity constant was extracted from these plots by fitting the precise model according to Piehler *et al*. (1997) to the data, assuming one-to-one stoichometry of the complex formation:

$$c_{\alpha 2} = \frac{c_{0,\alpha 2} - c_{0,R2} - K_d}{2} + \sqrt{\frac{(c_{0,\alpha 2} + c_{0,R2} + K_d}{4} - c_{0,\alpha 2} c_{0,R2}} \quad (2)$$

with the same parameters as defined in equation (1).

Stopped-flow measurements

Association rate constants were measured by monitoring de-quenching of tryptophan fluorescence upon interaction of IFNα2 and ifnar2-EC using a stopped-flow setup (Applied Photophysics SX-17MV). The excitation wavelength was 230 nm (Schreiber *et al*., 1994; slit width 1 mm) and emission was monitored using a cutoff filter of 320 nm. In each experiment, 400 data points were recorded over a reaction period of one to five seconds (at least five runs were averaged). Pseudo-first-order conditions during the interaction were provided by using at least a fivefold excess of IFNα2. The rates of the interaction k_s were determined from an exponential fit of the data. The association rate constant k_{on} was determined from a plot of k_s as a function of the IFNα2 concentration by linear regression.

The electrostatic contributions in the interaction between IFNα2 and ifnar2-EC were determined from association rate constants at salt concentrations between 0.025 M and 0.525 M NaCl. The relation between the electrostatic energy of interaction at the transition state U_{el} and the association rate constant k_{on} is given by:

$$\ln k_{on} = \ln k^0_{on} - \frac{U_{el}}{RT}\left(\frac{1}{1+\kappa a}\right) \quad (3)$$

where k^0_{on} is the basal rate of association in the absence of electrostatic forces, κ is the reciprocal Debye-Hückel screening length and a, which relates to the minimal distance of approach, was fixed to 6 Å. A plot of $(1+\kappa a)^{-1}$ *versus* $\ln k_{on}$ gives a linear corelation with a slope equal to U_{el}/RT, and an intercept at $\ln k^0_{on}$ (Schreiber & Fersht, 1996; Selzer & Schreiber, 1999; Vijayakumar *et al*., 1998).

Linear regression and non-linear least-squares fitting were done with Kalaidagraph software which calculates the standard error values of the parameters. Standard deviation for multiple measurements were determined using standard equations in Excel 5.0.

Acknowledgements

We thank M. Rubinstein and D. Novick for providing us with the cDNA of ifnar2-EC and for many helpful discussions, S. Barak for performing the IFN cytopathic effect assay, and Shira Albeck for her critical reading of the manuscript. We thank H.-M. Haake for his continous support setting up the RIfS system which was developed in the group of G. Gauglitz. This research was supported by grant number 96-00439/1 from the US - Israel Binational Science Foundation (BSF), Jerusalem, Israel. J.P. is an EMBO postdoctoral fellow, 1998.

References

Albeck, S. & Schreiber, G. (1999). Biophysical characterization of the interaction of the β-lactamase TEM-1 with its protein inhibitor BLIP. *Biochemistry,* 3811-3821.

Bignon, C., Sakal, E., Belair, L., Chapnik, C. N., Djiane, J. & Gertler, A. (1994). Preparation of the extracellular domain of the rabbit prolactin receptor expressed in *Escherichia coli* and its interaction with lactogenic hormones. *J Biol. Chem.* **269**, 3318-3324.

Cacaccia, P., Cletini, O., Isacchi, A., Bergonzoni, L. & Orsini, G. (1993). Biochemical characterization of the molecular interaction between recombinant basic fibroblast growth factor and a recombinant soluble fibroblast growth factor receptor. *Biochem. J.* **294**, 639-644.

Cohen, B., Novick, D., Barak, S. & Rubinstein, M. (1995). Ligand-induced association of the type I interferon receptor components. *Mol. Cell. Biol.* **15**, 4208-4214.

Cunningham, B. C. & Wells, J. A. (1993). Comparison of a structural and a functional epitope. *J. Mol. Biol.* **234**, 554-563.

Cutrone, E. C. & Langer, J. A. (1997). Contributions of cloned type I interferon receptor subunits to differential ligand binding. *FEBS Letters,* **404**, 197-202.

de Vos, A. M., Ultsch, M. & Kossiakoff, A. A. (1992). Human growth hormone and extracellular domain of its receptor: crystal structure of the complex. *Science*, **255**, 306-312.

Domanski, P., Witte, M., Kellum, M., Rubinstein, M., Hackett, R., Pitha, P. & Colamonici, O. R. (1995). Cloning and expression of a long form of the beta subunit of the interferon alpha beta receptor that is required for signaling. *J. Biol. Chem.* **270**, 21606-21611.

Fuh, G., Mulkerrin, M. G., Bass, S., McFarland, N., Brochier, M., Bourell, J. H., Light, D. R. & Wells, J. A. (1990). The human growth hormone receptor. Secretion from *Escherichia coli* and disulfide bonding pattern of the extracellular binding domain. *J. Biol. Chem.* **265**, 3111-3115.

Gauglitz, G., Brecht, A., Kraus, G. & Nahm, W. (1993). Chemical and biochemical sensors based on interferometry at thin (multi-)layers. *Sens. Act.* **11**, 21-27.

Gill, S. C. & von Hippel, P. H. (1989). Calculation of protein extinction coefficients from amino acid sequence data. *Anal. Biochem.* **182**, 319-326.

Harlos, K., Martin, D. M., O'Brien, D. P., Jones, E. Y., Stuart, D. I., Polikarpov, I., Miller, A., T, U. E. & Boys, C. W. (1994). Crystal structure of the extracellular region of human tissue factor. *Nature,* **370**, 662-666.

Karlsson, R., Michaelsson, A. & Mattsson, L. (1991). Kinetic analysis of monoclonal antibody-antigen interactions with a new biosensor based analytical system. *J. Immunol. Methods,* **145**, 229-240.

Langer, J. A., Yang, J., Carmillo, P. & Ling, L. E. (1998). Bovine type I interferon receptor protein BoIFNAR-1 has high-affinity and broad specificity for human type I interferons. *FEBS Letters,* **421**, 131-135.

Lewerenz, M., Mogensen, K. E. & Uze, G. (1998). Shared receptor components but distinct complexes for alpha and beta interferons. *J. Mol. Biol.* **282**, 585-599.

Loewenthal, R., Sancho, J., Reinikainen, T. & Fersht, A. R. (1993). Long-range surface charge-charge interactions in proteins comparison of experimental results with calculations from a theoretical method. *J. Mol. Biol.* **232**, 574-583.

Novick, D., Cohen, B. & Rubinstein, M. (1994). The human interferon alpha/beta receptor: characterization and molecular cloning. *Cell,* **77**, 391-400.

Piehler, J., Brecht, A. & Gauglitz, G. (1996). Surface modification for direct immunoprobes. *Biosens. Bioelectron.* **11**, 579-590.

Piehler, J., Brecht, A., Giersch, T., Hock, B. & Gauglitz, G. (1997). Assessment of affinity constants by rapid solid phase detection of equilibrium binding in a flow system. *J. Immunol. Methods,* **201**, 189-206.

Radhakrishnan, R., Walter, L. J., Hruza, A., Reichert, P., Trotta, P. P., Nagabhushan, T. L. & Walter, M. R. (1996). Zinc mediated dimer of human interferon-alpha 2b revealed by X-ray crystallography. *Structure,* **4**, 1453-1463.

Rubinstein, S., Familletti, P. C. & Pestka, S. (1981). Convenient assay for interferons. *J. Virol.* **37**, 755-758.

Schmitt, H. M., Brecht, A., Piehler, J. & Gauglitz, G. (1997). An integrated system for optical biospecific interaction analysis. *Biosens. Bioelectron.* **12**, 809-816.

Schoner, B. E., Belagaje, R. M. & Schoner, R. G. (1990). Enhanced translational efficiency with two-cistron expression system. *Methods Enzymol.* **185**, 94-103.

Schreiber, G. & Fersht, A. R. (1996). Rapid, electrostatic assisted, association of proteins. *Nature Struct. Biol.* **3**, 427-431.

Schreiber, G., Buckle, A. M. & Fersht, A. R. (1994). Stability versus function: two competing forces in the evolution of barstar. *Structure,* **2**, 945-951.

Selzer, Z. & Schreiber, G. (1999). Predicting the rate enhancement of protein complex formation from the electrostatic energy of interaction. *J. Mol. Biol.* **287**, 409-419.

Toniatti, C., Cabibbo, A., Sporena, E., Salvati, A. L., Cerretani, M., Serafini, S., Lahm, A. C., Ortese, R. & Ciliberto, G. (1996). Engineering human interleukin-6 to obtain variants with strongly enhanced bioactivity. *EMBO J.* **15**, 2726-2737.

Uzé, G., Lutfalla, G. & Gresser, I. (1990). Genetic transfer of a functional human interferon α receptor into mouse cells: cloning and expression of its cDNA. *Cell,* **60**, 225-234.

Uzè, G., Lutfalla, G. & Mogensen, K. E. (1995). α and β interferons and their receptor and their friends and relations. *J. Interferon Res.* **15**, 3-26.

Vijayakumar, M., Wong, K. Y., Schreiber, G., Fersht, A. R., Szabo, A. & Zhou, H. X. (1998). Electrostatic enhancement of diffusion-controlled protein-protein association: comparison of theory and experiment on barnase and barstar. *J. Mol. Biol.* **278**, 1015-1024.

Walter, M. R., Windsor, W. T., Nagabhushan, T. L., Lundell, D. J., Lunn, C. A., Zauodny, P. J. & Narula, S. K. (1995). Crystal structure of a complex between interferon-gamma and its soluble high-affinity receptor. *Nature,* **376**, 230-235.

Wang, Y., Shen, B. J. & Sebald, W. (1997). A mixed-charge pair in human interleukin 4 dominates high-affinity interaction with the receptor alpha chain. *Proc. Natl Acad. Sci. USA,* **94**, 1657-1662.

Edited by A. R. Fersht

(Received 30 December 1998; received in revised form 24 March 1999; accepted 24 March 1999)